

Sensitivity of the Isoscalar Giant Dipole Resonance to Optical Potentials

H. L. Clark, Y. -W. Lui and D. H. Youngblood

The isoscalar giant dipole resonance is of particular interest because its energy is related to the compressibility of nuclear matter [1]. We have previously reported [2,3] identification of this $3\leftarrow\bar{0}$ resonance in a number of nuclei. However our analysis also revealed significant excess E1 strength in the region of the isovector giant dipole resonance that might also be attributed to the isoscalar giant dipole resonance.

Therefore, in this work, we have investigated the sensitivity of the predicted cross section of the isovector giant dipole resonance (IVGDR) and the isoscalar giant dipole resonance (ISGDR) on the choice of optical model potentials for ^{90}Zr , ^{116}Sn , ^{144}Sm and ^{208}Pb . We have measured the elastic scattering of 240 MeV alpha particles on ^{90}Zr , ^{116}Sn [4], ^{144}Sm and ^{208}Pb out to rainbow angles and low-lying 2^+ and 3^- states out to large angles to better define the potentials in the nuclear interior and determined the proper optical potentials using a single folded alpha-nucleon form for the effective interaction [5].

Beams of 240 MeV alpha particles from the Texas A&M K500 superconducting cyclotron bombarded self-supporting ^{90}Zr , ^{144}Sm and ^{208}Pb foils mounted in the target chamber of the multipole-dipole-multipole spectrometer. The thickness of the targets were 3.80, 6.90 and 11.84 mg/cm², respectively, and all were enriched to >95%. The focal plane detector consisted of four 60 cm long proportional counters (separated by 13.55 cm) to measure x-position and θ , an ionization chamber to

measure ΔE , and a scintillator to measure E and to provide a fast trigger. The angle θ was calibrated by using a collimator with five 0.1° slit openings at -2, -1, 0, 1, and 2°. The principals of operation are similar to the detector described in Ref. [6].

The ^{208}Pb data were taken at spectrometer angles of 3.5, 5, 7, 9, 11, 13, 16, 19, 22, 26, 29, and 32° with a spectrometer acceptance of $\Delta\theta=\pm 2.0^\circ$ and $\Delta\phi=\pm 0.8^\circ$. The ^{90}Zr and ^{144}Sm data were taken during a later run at spectrometer angles of 4, 6, 8, 10, 12, 15, 18, 21, 25, 28 and 31° with a spectrometer acceptance of $\Delta\theta=\pm 2.0^\circ$ and $\Delta\phi=\pm 0.8^\circ$ and at 33° and 36° with a larger acceptance of $\Delta\theta=\pm 2.0^\circ$ and $\Delta\phi=\pm 2.0^\circ$. In the analysis, software cuts on θ were applied to divide each data set into ten angle bins, each corresponding to $\Delta\theta\approx 0.4^\circ$. The average angle for each bin was determined by averaging over the height of the solid angle defining slit and the width of the angle bin. For each angle bin, the elastic and inelastic scattering peak positions, widths, and cross sections were extracted by integration or by a Gaussian fitting routine. The elastic and inelastic scattering differential cross sections obtained are plotted versus average center-of-mass angle in Figs. 1 and 2. The error bars represent the combined uncertainty from statistical, systematic and angle error summed in quadrature. Absolute cross sections were obtained from the combination of charge integration, target thickness, solid angle, and dead time. Data from a monitor detector, fixed at $\theta_{\text{lab}}=20^\circ$, were used to verify the

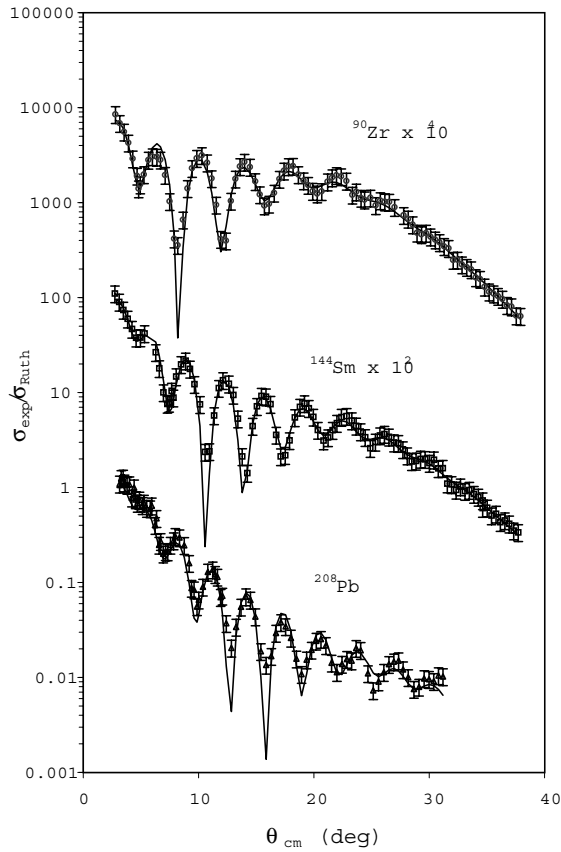


Figure 1. Angular distribution of the ratio of elastic scattering differential cross section to Rutherford scattering for 240 MeV α particles on ^{90}Zr , ^{144}Sm and ^{208}Pb plotted versus average center-of-mass angle. The folding model parameters used are those used in the ISGDR analysis of Ref. 9.

normalizations between the different data sets across the entire angular range. The experiment and analysis of the ^{116}Sn data are described in Ref. 4.

Optical model parameters were determined by fitting the data with the code PTOLEMY [7]. The folding model used to describe the interaction assumed a density-dependent, Gaussian-shaped, α -nucleon interaction to describe the real part of the potential and used a Woods-Saxon expression for the imaginary part of the potential. This form has been applied previously to describe 240

MeV alpha particle scattering of ^{58}Ni and ^{116}Sn and the details of the model and calculations with PTOLEMY are described thoroughly in Refs. [4,5]. Coupled-channel distorted-wave Born approximation (DWBA) calculations were carried out with PTOLEMY for the low-lying 2^+ and 3^- states. The expressions used for the sum rules and transition rates were obtained from Refs. [4,8].

The lines in Figs. 1 and 2 illustrate the differential cross sections calculated with the potentials used in our most recent analyses of the ISGDR in ^{90}Zr and ^{208}Pb [9]. The calculated differential cross sections for ^{116}Sn are shown in Ref. 4. The DWBA calculations for the low-

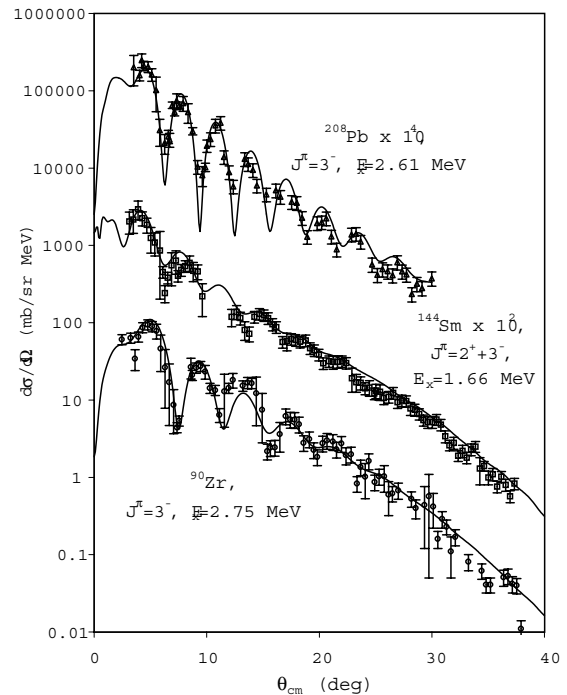


Figure 2. Inelastic scattering differential cross sections obtained for states indicated for ^{90}Zr , ^{144}Sm and ^{208}Pb excited by 240 MeV α particles plotted versus average center-of-mass angle. The calculations were made using the folding model parameters from Ref. [9] and accepted electromagnetic transition rates from Ref. [10].

lying 2^+ and 3^- states were normalized using accepted electromagnetic

strengths [10]. The figures show that the calculations, using these potentials, represent the differential cross sections of both the elastic and inelastic data quite well.

Different families of potentials were explored by adjusting the optical model parameters that provided good fits to parts and all of the elastic scattering data. It was found that the imaginary potential had the largest effect on the calculated ISGDR cross-section. If fits to the elastic data were made only at forward angles ($\theta < 15^\circ$), then the calculated ISGDR cross section could be wrong by a factor of 2 or more. It was also found that the calculated cross section of the IVGDR was insensitive to the choice of optical potentials. This is demonstrated in Fig. 3 that shows the result of fitting the full data set (solid line) and forward angle data set (dashed line) of elastic scattering for ^{208}Pb . Figures 3b and 3c show the corresponding ISGDR and IVGDR DWBA calculations made with these two families of potentials.

Using the presently accepted form for the transition density of the isoscalar giant dipole resonance [11], we have found the predicted cross section for the ISGDR to be very sensitive to the imaginary component of the optical and transition potential and particularly to the potential in the interior of the nucleus. Therefore, if the optical potential is determined only from the diffractive region of elastic scattering, the differential cross section for the ISGDR can differ by large amounts for different families of potentials, which provide acceptable fits to the elastic scattering data. An incorrect representation of the optical potential can have a dramatic effect on the extracted strength of the ISGDR as well as the extracted centroid energy and the resulting value for the nuclear matter

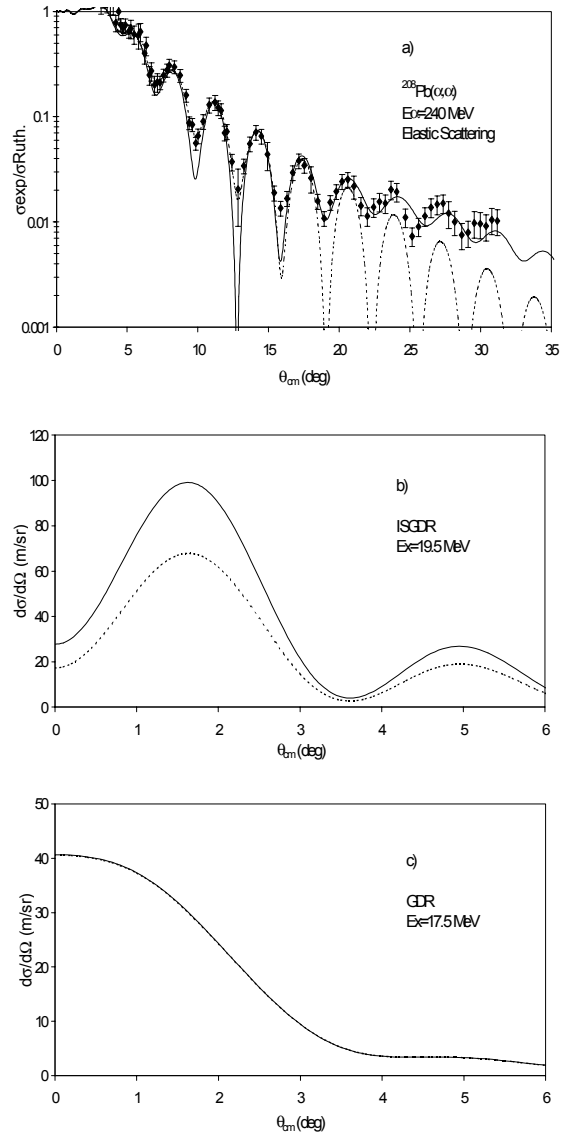


Figure 3. a) Calculated elastic scattering cross sections with optical potentials determined from fits to the full data set (solid line) and forward angle data set (dashed line), $\theta < 15^\circ$, for ^{208}Pb . b) and c) Calculated cross sections for the ISGDR and IVGDR using the two families of optical potentials determined from the elastic scattering fits described in a). The solid and dashed lines are indistinguishable in c).

incompressibility. A correct representation for the optical potential can be determined by analyzing the elastic scattering cross section over a large angle range up to rainbow angles,

using the folding model to describe the projectile-nucleus interaction. Calculating the cross sections for low-lying states and comparing the deduced transition rates with electromagnetic values can further test the optical potential. The calculated cross section for the IVGDR was found to be insensitive to the optical potential since the excitation is dominated by Coulomb excitation.

With the improved folding model parameters determined by this work, our most recent analysis of the ISGDR in ^{90}Zr , ^{116}Sn and ^{208}Pb excited by 240 MeV alpha scattering [9] has confirmed that the resonance is split into two components located at $\sim 72/A^{1/3}$ and $\sim 114/A^{1/3}$. The upper component is the compression mode and was found to exhaust $\sim 100\%$ of the E1 energy-weighted sum rule (EWSR) in each nuclei. The lower component is believed to be a new mode as suggested by random phase approximation-Hartree Fock and relativistic mean field theory calculations [12-14] and was found to exhaust $\sim 30\%$ of the E1 EWSR in each nuclei.

References

- [1] S. Stringari, Phys. Lett. **108B** (1982) 232.
- [2] H. L. Clark, Y. -W. Lui, D. H. Youngblood B. Kharraja, M. N. Harakeh and N. Kalantar-Nayestanaki, Nucl. Phys. **A649** (1999) 57.
- [3] D. H. Youngblood, H. L. Clark and Y. -W. Lui, RIKEN Review No. 23 (July, 1999) 159.
- [4] H. L. Clark, Y. -W. Lui and D. H. Youngblood, Phys. Rev. C **57** (1998) 2887.
- [5] G. R. Satchler and Dao T. Khoa, Phys. Rev. C **55** (1997) 285.
- [6] D. H. Youngblood, Y. -W. Lui, H. L. Clark, P. Oliver, and G. Simler, Nucl. Instr. Meth. Phys. Res., Sect. **A361** (1995) 539.
- [7] M. Rhoades-Brown, M. H. Macfarlane, and S. C. Pieper, Phys. Rev. C **21** (1980) 2417; 2436; M. H. Macfarlane and S. C. Pieper, Arg. Nat. Lab. Rep. No. ANL-76-11, Rev. 1 (1978).
- [8] G. R. Satchler, Nucl. Phys. **A472** (1987) 215.
- [9] H. L. Clark, Y. -W. Lui and D. H. Youngblood, Phys. Rev. C (2000) submitted.
- [10] NNDC Nuclear Data Tables, Brookhaven National Laboratory.
- [11] M. N. Harakeh and A. E. L. Dieperink, Phys. Rev. C **23** (1981) 2329.
- [12] A. Kolomietz, O. Pochivalov and S. Shlomo, *Progress in Research*, Cyclotron Institute, Texas A&M University (1998–1999).
- [13] D. Vretenar, A. Wandelt and P. Ring, Phys. Lett. **B487** (2000) 334.
- [14] G. Colo, N. Van Giai, P. F. Bortignon and M. R. Quaglia, Phys. Lett. **B485** (2000) 362.